Supplementary Information (SI) for

Intercomparison of detection and quantification methods for methane emissions from the natural gas distribution network in Hamburg, Germany

Hossein Maazallahi[1 2], Antonio Delre[3], Charlotte Scheutz[3], Anders M. Fredenslund[3], Stefan Schwietzke[4], Hugo Denier van der Gon[2], Thomas Röckmann[1]

[1]*Institute for Marine and Atmospheric research Utrecht (IMAU), Utrecht University (UU), Utrecht, The Netherlands*
[2]*Netherlands Organisation for Applied Scientific Research (TNO), Utrecht, the Netherlands*
[3]*Department of Environmental Engineering, Technical University of Denmark (DTU), Lyngby, Denmark*
[4]*Environmental Defense Fund (EDF), Berlin, Germany*

Correspondence: Hossein Maazallahi (h.maazallahi@uu.nl)

This section includes:
Supplementary Text
Supplementary Tables S1 to S8
Supplementary Figures S1 to S12

Table of Contents

S.1) Measurement intercomparison planning V
S.2) Emission outlets XII
S.3) Leak detection, confirmation and attribution XIV
S.4) Leak quantification methods XV
S.4.1) Mobile method XV
S.4.2) Tracer method XVI
S.4.3) Suction method XVIII
S.4.4) Gas leak quantification based on hole models XIX
S.5) Gas leak detection and quantification methods overview XX
S.5.1) Detection and attribution of locations XX
S.5.1) Quantifications of locations XXI
S.6) Gas leak influence on urban vegetation XXIII
S.7) Leak localization XXIV
S.8) Comparison of two CRDS instruments, G2301 and G4302 XXV
S.8.1) Comparison of maximum CH_4 enhancements and plume area XXV
S.8.2) Detection of leak indications with two instruments XXV
S.8.3) Emission quantification comparisons XXVI
S.9) Impact of distance on the enhancements XXVIII
S.10) Use of 10% or 10 ppb threshold XXIX
S.11) Descriptions of locations that were not described in detail in the main text XXX
S.11.1) HH003 XXX
S.11.2) HH004 XXXI
S.11.3) HH005 XXXII
S.11.4) HH006 XXXIII
S.11.5) HH009 XXXIV
S.11.6) HH010 XXXV
S.11.7) HH012 XXXVI
S.11.8) HH013 XXXVII
S.11.9) HH014 XXXVIII
S.11.10) HH015 XXXIX
S.11.11) HH100 XL
S.11.12) HH102 XLI
S.11.13) HH103 XLII
S.11.14) HH104 XLIII

List of Tables

Table S1 - Measurement matrix of method intercomparison campaign in Hamburg.....VI

Table S2 - Example of mobile measurements transects at one of the locations XV

Table S3 - Overview of all measurements performed with the tracer release method XVI

Table S4 - Attribution of individual plumes from mobile measurements using C_2H_6 and CO_2 signals XX

Table S5 - Measurement overview of the mobile, tracer and suction methods XXI

Table S6 - Observation comparison of CH_4 enhancements from G2301 and G4302 XXV

Table S7 - Emission quantification comparison with two different instruments. The G2301 is similar to the instrument that was used to derive the conversion equation (Eq. 1 in the main manuscript, Weller et al, 2019). The G4302 has a much shorter sample exchange time of the measurement cell, therefore, higher enhancements, which translate to higher emission rates if the same conversion equation (Eq. 1) is used for quantification. XXVI

Table S8 - Emission estimate for the C_2H_2 release rate from 5 mobile quantifications in the tracer release technique. These were evaluated a) with the original 10% (≈ 200 ppb) threshold and b) with a 10 ppb threshold. The lower threshold was still applied in order to exclude transects where the plume is completely missed. XXIX

List of Figures

Figure S1 - Variety of emission outlets detected in Hamburg XIII

Figure S2 - Example of a visit at one of the locations, HH008, together with the LDC XIV

Figure S3 - Drilling holes around the surface-projected track of gas pipeline (a) and measuring the CH4 mole percentage (b) to find the gas leak location, HH008 XIV

Figure S4 - Mobile measurements vehicle XV

Figure S5 - Tracer method in static mode (a) at HH004 and in mobile mode (b) at HH014 XVI

Figure S6 - Results from the tracer method applied in static (top panel, HH001) and mobile (bottom panel, HH014) modes. XVII

Figure S7 - Inserting suction probes into holes drilled above the pipeline at location HH009 (a), and quantification in action at location HH002 (b). XVIII

Figure S8 - Example of unhealthy trees (red box) affected by a gas leaks in close vicinity, HH004 (a) and HH010 (b) XXIII

Figure S9 - The LDC reported 6 leaks on the pipeline at this location with total leak area of 5 cm^2, HH013 XXIV

Figure S10 - comparison between maximum CH4 enhancements (a) and plume areas (b) from two different instruments, G2301 and G4302. XXV

Figure S11 - Emission comparison between the two CRDS instruments, G2301 and G4302, onboard the mobile measurement vehicle XXVII

Figure S12 - Impact of distance on the measurements during mobile measurements XXVIII

S.1) Measurement intercomparison planning

In this intercomparison campaign, participating teams from Utrecht University (UU), Technical University of Denmark (DTU) and EON joined the local host of Gasnetz Hambug (GNH). UU applied the mobile detection and quantification methods, DTU the tracer release method and EON deployed the suction method, and GNH contributed to the leak detection or confirmation and applied gas leak repair protocols. In total, the four teams spent about 6 weeks to first detect and then quantify gas leaks. In the process of planning the intercomparison campaign, all participants contributed to a method intercomparison matrix, where the characteristics of the different measurement approaches were compared (Table S1). The matrix includes descriptions related to the identification of gas leaks, the quantification of gas leaks, adjustments of the method to the intercomparison exercise and upscaling. It also laid out an initial plan for the intercomparison project in terms of identification of suitable locations and deployment of the different methods. This plan was based on the expectation that we would ideally be able to locate 50 leak locations in preparatory mobile surveys from UU, supplemented with locations from routine leak detection surveys by the Local Distribution Company (LDC). Out of 50 leak locations, 10 leak locations would be selected for the intercomparison, ideally including at least 3 locations from each of the three emission categories (low/medium/high) as used by the mobile evaluations (von Fischer et al., 2017; Maazallahi et al., 2020). Emissions at these locations would subsequently be quantified by the tracer release and suction teams. This approach failed for two reasons: (i) it was not possible to locate 50 leak indications (LIs) in the preparatory surveys in August 2020 and (ii) several of the leak locations had to be fixed immediately or within a week of detection (A1 or A2 category). In one example, gas leak emission rate was estimated about 5.0 L min^{-1} from the mobile method. Therefore, in a second attempt in September 2020, all the three teams were in Hamburg at the same time to immediately quantify any confirmed locations just before repair.

Table S1 - Measurement matrix of method intercomparison campaign in Hamburg

Mobile Method		
Site Selection	**Approach**	• Random sampling of leak indications • Extensive coverage of large fraction of the street network (potentially in target areas within city) • Partial (or complete in the US) re-sampling for verification So far usually one-time, multi-week intensive field campaign
	Adjustment for inter-comparison	• Stratified random sampling of LIs • For the intercomparison it would be good if we observe a larger number (≈ 50) of LIs with a "representative" distribution, i.e. including LIs from three categories (low/med/high leak rate). Possible to include LIs indicated by the carpet method during previous service walks (this would not be random, but an additional targeted survey to increase database) • Based on the population of LIs found, select 10 LIs for intercomparison with the suction method, including three per category (low/med/high leak rate) • Low leak rates are those below 6 L min^{-1} (= 360 L h^{-1}), medium between 6 and 40 L min^{-1} (= between 360 and 2.400 L h^{-1}) and high is everything above 40 L min^{-1} (2.400 L h^{-1}). • If not enough LIs from all categories are found: select 10 sites with a variation of assumed leak sizes from the 'collection' found. • Further identification of leak locations using carpet method (part of the standard leak survey) and portable Picarro instrument if needed • Possibility to prioritize locations previously identified by carpet method
Air Sampling	Site preparation	n/a
	Measurement process	• Air inlet at front bumper or roof of vehicle • Methane concentration measurement in instrument inside the vehicle • GPS determines location where methane plume entered inlet (inlet/instrument delay accounted for)
	Further Conditions	• Quantification is not reliable under no wind or stormy conditions. There are no formal thresholds on when the method can be applied, so decisions will be taken based on scientific judgement during the campaign. During poor wind conditions we would still attempt to identify LIs for creating our population, to be quantified later during more suitable conditions. • Fresh rain fills the soil pores and will block methane diffusion out of the soil, so mobile surveys will not be carried out during/shortly after mid to strong rain events.
Leak-level analysis	Flux quantification	• Conversion of methane concentrations to flux using regression model based on controlled release field experiments

	Flux interpretation	• Estimates for individual locations have considerable flux uncertainties • This necessitates large sample size to reduce city-level flux uncertainties • Quantified flux at a given LI location are from plumes released to atmosphere
	Identification of location	• Localization of approximate leak expression (within 30 m)
Spatial extrapolation		• Method produces information about LIs per km, leak rates per km, taking into account repeats and spatial aggregation • Can be extrapolated to total length of road network within city boundaries • Extrapolation to other cities or country scale possible, but has high uncertainties (very big differences between different cities in US) • Extrapolation to country scale may require more measurements in different cities and/or identification of suitable parameter (activity value) for upscaling
	Interpretation	• Accuracy of extrapolation depends on the representativity of surveyed city section (in terms of pipeline age, material, etc.) to the extrapolated area. Accuracy increases with knowledge of pipeline infrastructure in the surveyed and extrapolated area (and accounting for this knowledge in the model).
Tracer Method		
Site Selection	**Approach**	• Not a typical method for gas distribution leak emission quantification, thus approach will be designed specifically for inter-comparison project (see below)
	Adjustment for inter-comparison	• Same sites that will also be quantified using suction / carpet method. • Note possible interference of other nearby CH_4 sources.
Air Sampling	Site preparation	• Need access downwind at moderate distance (e.g., more than 10 m, less than 100 m) • Need to be able to safely release tracer gas at leak expression location
	Measurement process	• Tracer gas released at known rate at outlet(s) • Methane concentration and tracer gas measurements measured downwind of source with vehicle-mounted instruments

	Further Conditions	• Quantification with the tracer method requires adequate meteorological conditions. The expert group from DTU will assess this during the surveys.
Leak-level analysis	Flux quantification	• Flux estimation based on ratio of tracer gas to CH_4 and the known tracer gas release rate
	Flux interpretation	• Uncertainty: < 20% (Fredenslund et al., 2019) under normal operating conditions • Quantified flux at a given LI location are from tracer released to atmosphere
	Identification of location	• n/a (location was known before)
Spatial extrapolation		• Tracer method not meant to be spatially extrapolated to city-level • For inter-comparison project, objective of tracer method is to provide comparison for emission quantification from *individual* leak locations
	Interpretation	See above
Suction Method		
Site Selection	**Approach**	• No selection of an existing "leak pool" since leaks are repaired after they were detected by the operator → cooperation with the grid operators is necessary to intervene the process and make the measurement possible • Leaks from underground pipes found during standard leak survey are being reported using an initial protocol. Leaks reported this way are being measured 'as they come', as finding leaks takes time and leaks found soon need to be repaired with respect to DVGW rules. Thus, it is not possible to collect a larger number of leaks to choose from first. • Standard leak survey in Germany follows technical rulebook G465 of the DVGW in which both periods of time are specified with respect to pipeline pressure, material and history of leak rate per km as well as the actual survey procedure. Basically, a fraction of a DSO's grid is surveyed every year and the areas to be covered are planned in advance for every year. Then specialized employees or a service provider (both have to be certified/trained with respect to G465; today having a service provider do the survey is very common) are walking along the pipes using maps with documentation of the pipeline positions. To trace natural gas emissions from the ground both a

		visual inspection (for example checking for faded vegetation along the pipeline trace) and concentration measurements using equipment allowed/specified by G465 are applied. Equipment used for concentration measurements with a ppm resolution are either FIDs (flame ionization detector) or semiconductor detectors. Indications found must be reported using standardized templates the DSO uses later on to decide on further actions. If a leak of category AI or AII is found the DSO is informed immediately to start repairs asap (refer to annex for explanation on risk categories). • After accessing the suitability for measurement (enough time for preparation – i.e. a leak that does not have to be repaired immediately, accessible surroundings – e.g. not in the middle of a heavy traffic road or on private property the DSO lacks permission to enter, enough space for equipment, project wise to make sure that different types of leak situations – like pressure level, pipeline material, rural vs. urban environment, pipe diameter, location distribution across Germany – are being reflected) a measurement is scheduled. • Any interested DSO can report a leak for examination. In this regard there is a certain level of randomness.
	Adjustment for inter-comparison	• If possible: minimum 3 sites per category (low/med/high leak rate) defined by mobile measurements (definition ref. column right) • If not possible: 10 sites with a variation of assumed leak sizes from the 'collection' found, maybe not covering all leak size categories. • General site areas determined by mobile method stratified sampling • Further identification of leak locations using carpet method (part of the standard leak survey) and portable Picarro instrument if needed (i.e., if carpet is unable to detect the leak)
Air Sampling	Site preparation	• Need to be able to bring measurement equipment to site (by car); enough space to place equipment. • Localization of leaks has taken place upfront. • If leak is close to a street there needs to be barriers
	Measurement process	• Freeing soil above assumed leak location from potential excess methane accumulations by sucking air from the soil through up to 12 probes at approx. 35 cm depth until methane concentration equilibrium is reached in the soil. • Measurement of air flow rate (via flow meter) and methane concentration (via FID).
	Further Conditio	• Rain dependency: not possible when soil is soaked with rain • Wind dependency: none • Temperature dependency: not possible when soil is frozen
Leak-level analysis	Flux quantificati	• Calculation of leak rate from pipe to soil by combining measured values for both methane concentration and volume flow in air-gas-mixture sucked through the soil after equilibrium is reached.
	Flux interpretation	• Measurement of flux into the soil at specific location(s) where leaks were previously identified using the standard leak survey. • Since information of the location of the pipeline is available and additional probing holes will be drilled to specify the leak site along other quality assurance measures it is seen as unlikely to measure a false-positive this way.

		• Uncertainties range at ± 10% based on 23 measurement points on two independent test sites with artificial leaks allowing to create controlled release rates at E.ON Ruhrgas and Gaz de France as part of a GERG project conducted in the mid-1990s.
	Identification of location	• n/a (location was known before) • Nevertheless, localization is checked at the beginning of the measurements based on above-ground methane concentrations measured via carpet/bell probe at drilling holes.
Spatial extrapolation		• Spot sample is extrapolated to national/country-specific emission factors for leaks of underground pipes • Knowing the pipeline material and operation pressure of each spot sample, when applied at sufficiently large sample size (N >> 10), statistical analysis will tell if emission factors can be differentiated by e.g. pipeline material or operation pressure. Emission factors are being derived from full measurement campaign within DVGW's ME-DSO project, NOT based on measurements in Hamburg alone! • Aggregation of emissions is done via MEEM method (ref. link) • MEEM distinguishes in detail between several different leak sources with corresponding ways to access and accumulate data. (Please refer to annex for a tree diagram illustrating all different source paths covered by MEEM. These include leaks detected by survey, incidents and operational emissions as well as leaks reported by third parties for both pipelines and facilities. In the Hamburg campaign only the path "leaks detected by survey" is being investigated.) • For underground leaks an event-based approach is foreseen • DVGW is collecting data on leaks found through survey from all national gas grid operators (GaWaS) – these are categorized by safety risks (A1, A2, B, C – for definitions see below) • Principal formula: E_CH4 = EF * n * t, where EF is the emission factor for underground leaks [l_CH4/h], n is the number of leaks this EF applies to and t is the assumed average lifetime [h] of such a leak • Category-specific lifetimes of leaks/incidents: Average lifetimes for leaks found in a survey are retrieved via t = (t_period + t_repair)/2, where t_period is the timespan in which a respective segment of pipe (depending on material, pressure, leak frequency history) needs to be surveyed and t_repair is the maximum time needed to repair a leak of the respective category. The calculation is a naïve statistical average as the leak might occur immediately after the last time the respective pipe segment has been surveyed or just before the survey takes place. • Conservative lifetime estimate: Maximum repair times for each category can be found via the DVGW rulebook while many DSOs will repair most leaks a lot quicker • More realistic approach: average repair time per category is known by operator and used in calculation • As regular surveys in a year will not cover the entire pipeline length a rolling horizon over a survey period needs to be considered (average leak lifetimes are in the range of 2,25 years for leaks checked every four years for example, hence calculations over four years should be averaged)

	Interpretation	• Accuracy of aggregation depends on quality of EF and completeness of leak identification through surveys • In Germany, the spatial extrapolation assumes that the vast majority of all existing leaks will be found through survey • The EF is being derived from spot sampling where all kinds of circumstances existing in the national distribution grid is supposed to be represented. As it is intended to split emission factors by statistically relevant parameters such as e.g. pipeline material changes in the structure of the grid can be accounted for. • This can also be applied if aggregated emission values for a single DSO or grid are wanted. The respective structure of the grid under consideration can be mimicked by separating number of leaks with respect to parameters different EFs apply for. • The MEEM method comprises of a lot more categories (other intrinsic emissions such as permeation from plastic pipes, operational emissions from maintenance, repair, construction and dismantling and incident emissions e.g. from digging accidents) than just underground pipes to compile a complete emission value that can be retrieved on different levels (single grid, entire grid of a DSO, national view).

S.2) Emission outlets

Figure 1 shows example of outlets that were identified in this study. A manhole next to a tree (a, HH009), a manhole in the middle of street (b, HH005), asphalt cracks (c, HH101), rain drains (d, HH009), a hydrant (e, HH010), a vent (f, HH011), bare soil surface next to a street (g, HH012), bare soil surface next to a tree (h, HH003), a cobble stone street (i, HH001), gaps between street curbs (j, HH006), surface gas caps on top of gas pipelines (k, HH100), telecommunication cover on streets (l, HH004), open ground before repair (m, HH014). Fig. S1n shows one of the examples when a leak had to fixed before quantification could be applied (black pipeline).

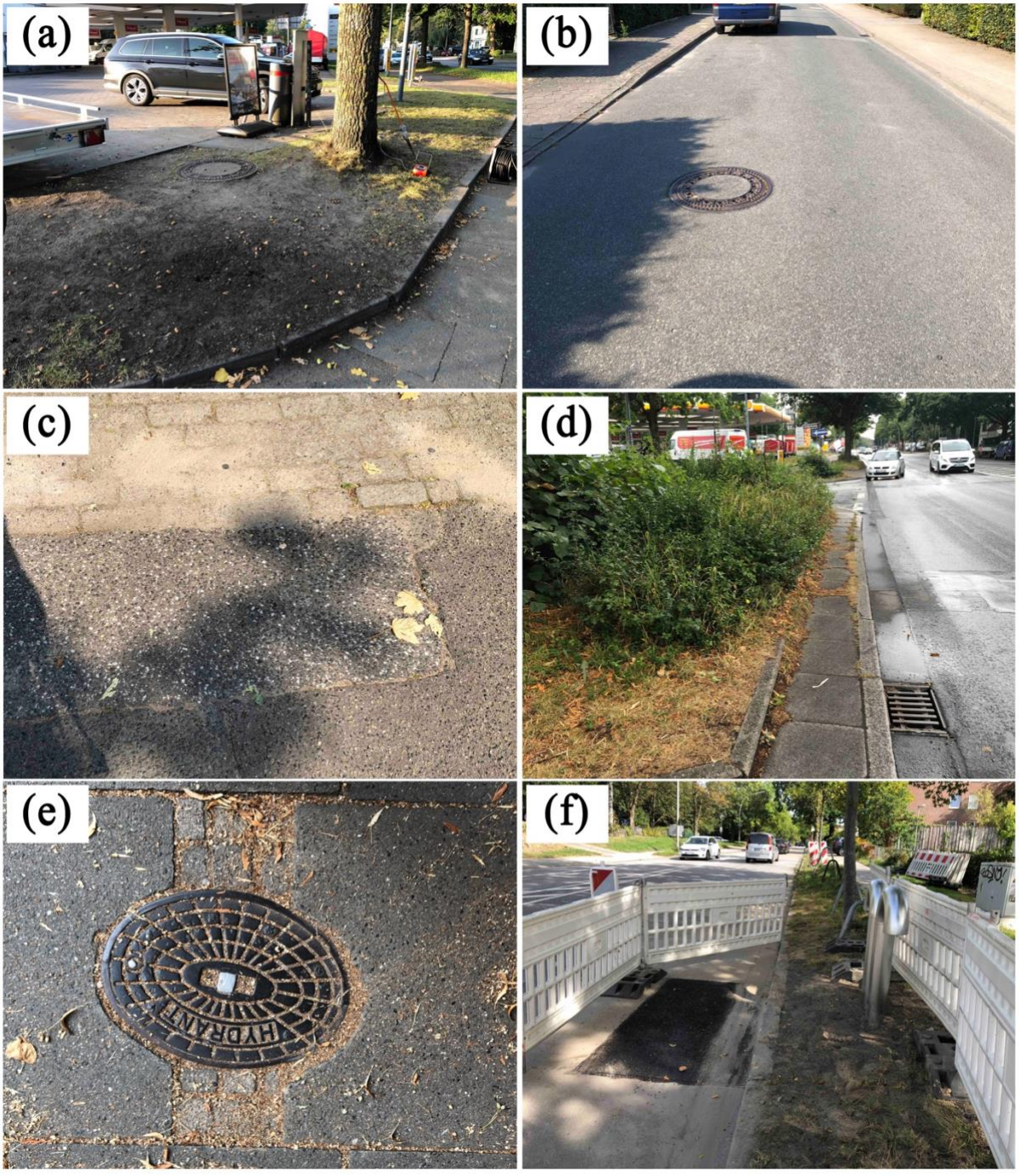

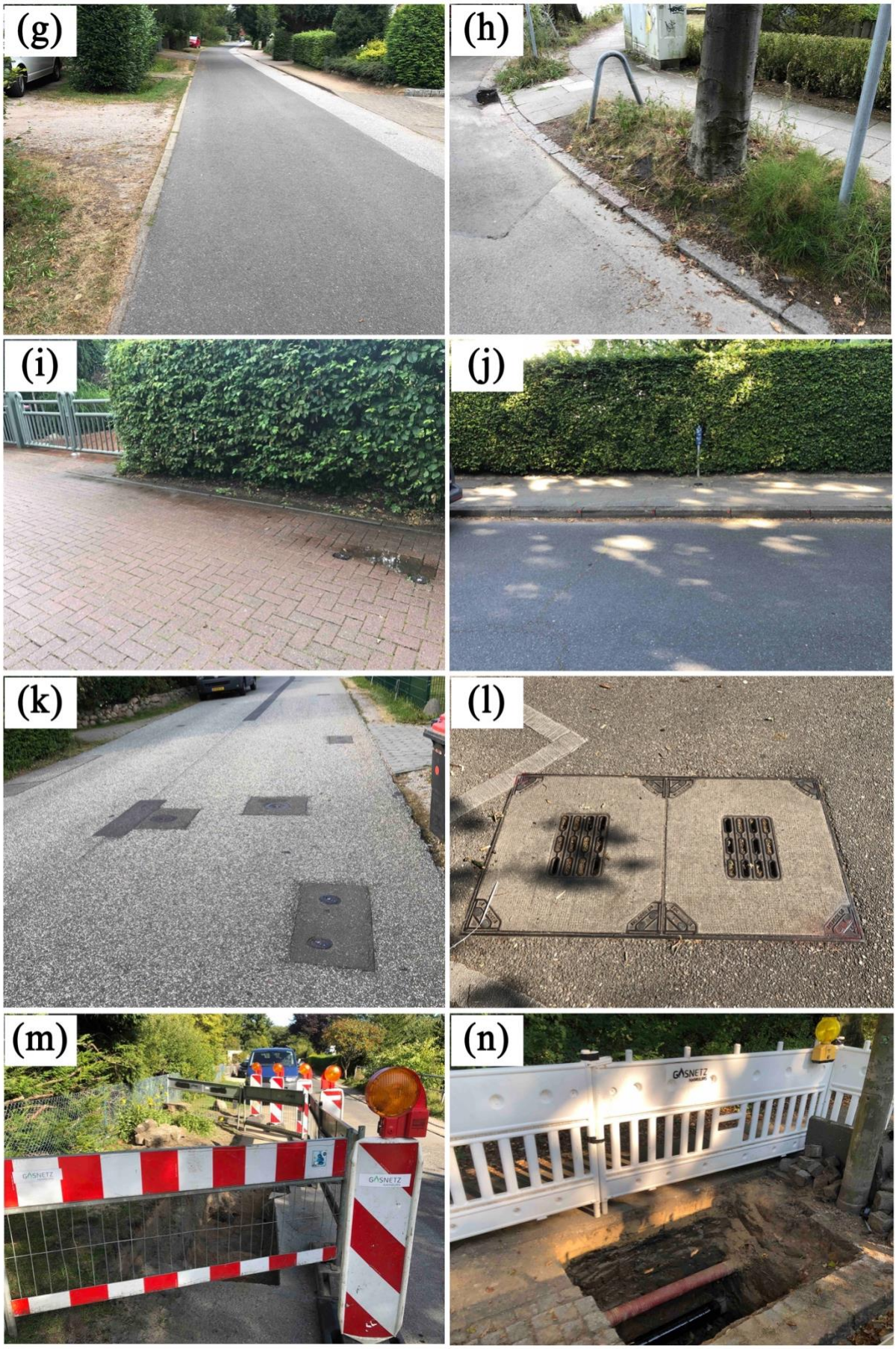

Figure S1 - Variety of emission outlets detected in Hamburg

S.3) Leak detection, confirmation and attribution

In this campaign we focused on 15 locations which were initially detected by mobile surveys and later confirmed as gas leaks by the LDC, except for 2 locations, plus 5 more locations which had been already detected by the LDC leak detection surveys. After sharing the locations with the LDC we visited the locations with the leak searching experts from the LDC (Fig. S2). When a leak had been confirmed, the LDC leak searchers drilled holes (Fig. S3a) and measured subsurface CH_4 volume mole fraction for each hole (Fig. S3b).

For the mobile measurements, we used carbon dioxide (CO_2) and ethane (C_2H_6) signals to attribute methane (CH_4) signals. From our past experiments (Maazallahi et al., 2020), we concluded that combustion signals in Hamburg are mostly related to engine combustion. Microbial emissions were sometimes, but not always, also associated with CO_2 signals. We considered a microbial contribution to the observed CH_4 enhancement if the linear regression of CH_4 and CO_2 enhancements had $R^2 > 0.8$. To evaluate the CO_2:CH_4 ratio, the start and end point of CH_4 enhancements were defined when the mole fraction increased 20 ppb above background level until it dropped below the 20-ppb enhancement again. If we observed CO_2 signals associated with CH_4 and with ethane to methane ratio (C_2:C_1) less than 10% we attributed those signals a to mixed plume of fossil and microbial emissions.

Figure S2 - Example of a visit at one of the locations, HH008, together with the LDC

Figure S3 - Drilling holes around the surface-projected track of gas pipeline (a) and measuring the CH4 mole percentage (b) to find the gas leak location, HH008

S.4) Leak quantification methods

S.4.1) Mobile method

Figure S4 - Mobile measurements vehicle

Table S2 shows an example of a location, HH001, where we performed 10 transects. For this location all the transects were accepted for the quantification (1 for accepted and 0 for denied), and on all the transects the status of the two instruments indicated proper operation (1 for running properly and 0 for malfunctions).

Table S2 - Example of mobile measurements transects at one of the locations

ID	Transect No.	Transect	G2301 status	G4302 status	Date (dd.mm.yyyy)	Start_UTC (hh:mm:ss)	End_UTC (hh:mm:ss)
HH001	1	1	1	1	21.08.2020	09:24:10	09:24:35
HH001	2	1	1	1	21.08.2020	09:29:45	09:30:54
HH001	3	1	1	1	21.08.2020	09:54:43	09:55:21
HH001	4	1	1	1	21.08.2020	09:59:01	09:59:33
HH001	5	1	1	1	22.08.2020	11:44:17	11:44:47
HH001	6	1	1	1	22.08.2020	11:45:31	11:45:59
HH001	7	1	1	1	13.09.2020	13:11:34	13:12:10
HH001	8	1	1	1	13.09.2020	13:39:10	13:39:54
HH001	9	1	1	1	14.09.2020	12:52:09	12:52:39
HH001	10	1	1	1	14.09.2020	12:55:38	12:56:13

S.4.2) Tracer method

Table S3 - Overview of all measurements performed with the tracer release method

ID	Tracer method; Mobile (M), Static (S)	Date (dd.mm.yyyy)	Time_Start (hh:mm:ss)	Time_End (hh:mm:ss)	Distance between CH_4 maxima and release point (m)	Distance of release to the leak location (m)	Wind Speed ($m\ s^{-1}$)
HH001	S	23.092020	15:01:09	15:43:28	≈ 30	< 1	0.3
HH002	S	23.09.2021	13:58:42	14:30:24	≈ 40	≈ 6	0.5
HH003	S	22.09.2020	08:27:57	09:14:30	≈ 25	≈ 5	0.3
HH004	S	23.09.2020	11:53:00	12:24:05	≈ 40	≈ 5	0.6
HH005	S	20.09.2020	17:11:40	18:09:17	≈ 40	-	-
HH006	S	25.09.2020	11:22:07	11:49:41	≈ 15	≈ 3	0.5
HH007	-	-	-	-	-	-	-
HH008	M	21.09.2020	09:28:00	10:33:00	≈ 35	≈ 1	-
HH009	M	21.09.2020	13:58:00	15:56:00	≈ 43	≈ 20	0.5
HH010	M	22.09.2020	13:16:00	14:56:00	≈ 44	≈ 4	0.6
HH011	M	24.09.2020	07:54:00	08:50:00	≈ 35	≈ 64	1.95
HH012	-	-	-	-	-	-	-
HH013	-	-	-	-	-	-	-
HH014	M	20.09.2020	14:24:00	15:08:00	-	< 1	-
HH015	S	25.09.2020	09:37:33	10:18:52	≈ 20	≈ 3	0.9
HH100	S	24.09.2020	10:55:13	11:26:33	≈ 30	≈ 2	2.5
HH101	S	25.09.2020	13:55:06	14:33:36	≈ 15	≈ 4	0.6
HH102	S	24.09.2020	15:19:37	16:07:41	≈ 20	≈ 3	-
HH103	S	24.09.2020	12:19:30	13:10:51	≈ 18	< 1	-
HH104	-	-	-	-	-	-	-

Figure S5 - Tracer method in static mode (a) at HH004 and in mobile mode (b) at HH014

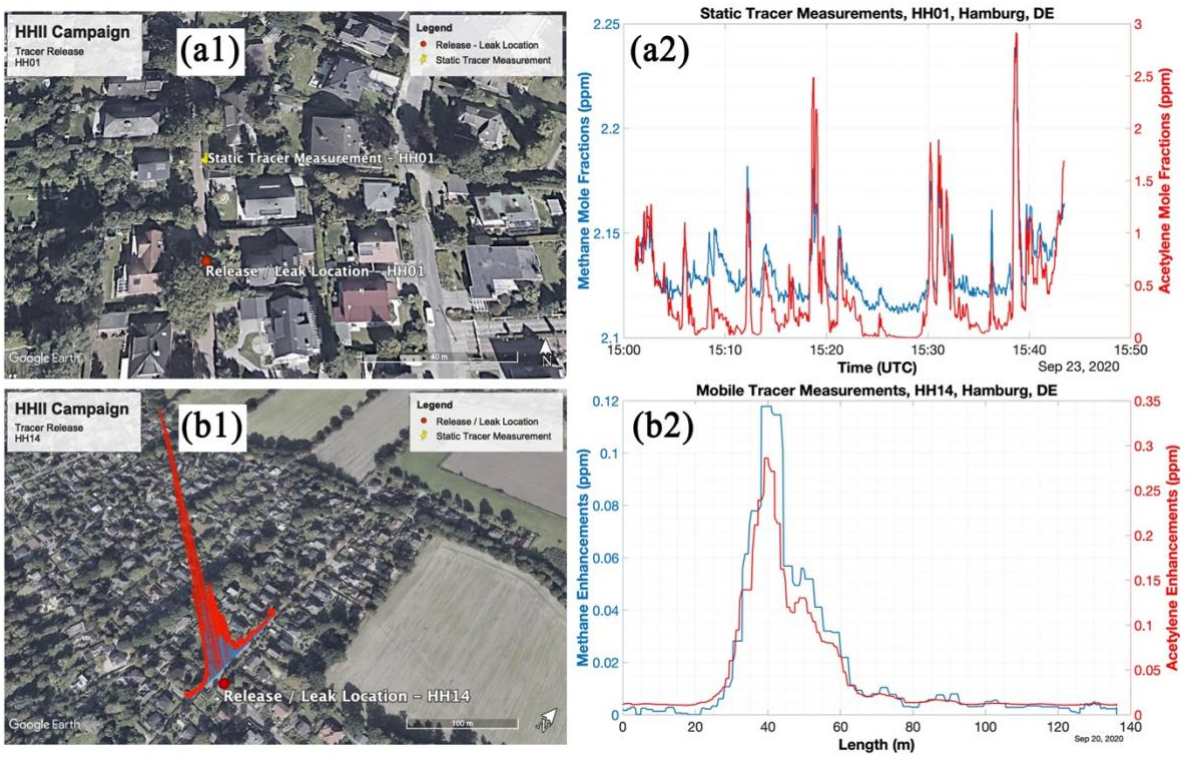

Figure S6 - Results from the tracer method applied in static (top panel, HH001) and mobile (bottom panel, HH014) modes, aerial images: © Google Maps.

S.4.3) Suction method

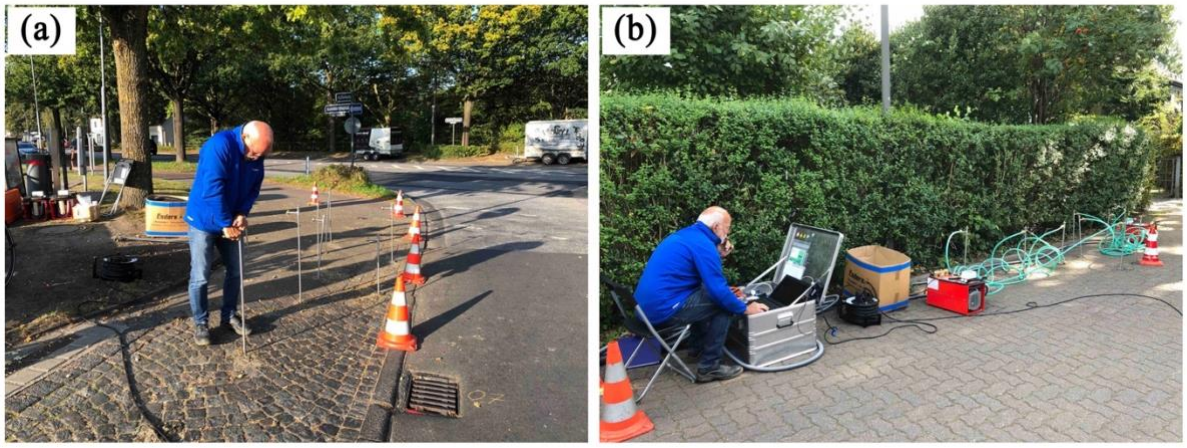

Figure S7 - Inserting suction probes into holes drilled above the pipeline at location HH009 (a), and quantification in action at location HH002 (b).

S.4.4) Gas leak quantification based on hole models

There are several models to quantify CH4 emissions from a pipeline in open space or underground. Equation S1 was developed by Ebrahimi-Moghadam either for the pipeline leaks in open space (Eq. S1a) or for buried pipelines (Eq. S1b). In this model, β is the ratio of hole diameter to pipeline diameter, d is the hole diameter in mm, and p is the pipeline absolute pressure in bar and Q is in $m^3\ hr^{-1}$.

$$\boldsymbol{Q} = \begin{cases} \mathbf{0.808} * \left(\mathbf{1} + \boldsymbol{\beta}^{\mathbf{4}}\right) * \boldsymbol{d}^{\mathbf{2}} * \boldsymbol{p}, & \boldsymbol{d} \leq \mathbf{15}\ \boldsymbol{mm} \\ \mathbf{0.708} * \left(\mathbf{1} + \boldsymbol{\beta}^{\mathbf{4}}\right) * \boldsymbol{d}^{\mathbf{2}} * \boldsymbol{p}, & \mathbf{15} < \boldsymbol{d} \leq \mathbf{80}\ \boldsymbol{mm} \end{cases} \quad \textbf{Eq. S1a}$$

$$\boldsymbol{Q} = \begin{cases} \mathbf{0.117} * \left(\mathbf{1} + \boldsymbol{\beta}^{\mathbf{4}}\right) * \boldsymbol{d}^{\mathbf{2}} * \boldsymbol{p}, & \boldsymbol{d} \leq \mathbf{15}\ \boldsymbol{mm} \\ \mathbf{0.0677} * \left(\mathbf{1} + \boldsymbol{\beta}^{\mathbf{4}}\right) * \boldsymbol{d}^{\mathbf{2}} * \boldsymbol{p}, & \mathbf{15} < \boldsymbol{d} \leq \mathbf{80}\ \boldsymbol{mm} \end{cases} \quad \textbf{Eq. S1b}$$

In the model from Cho et al. (2020), gas leak emission rates depend on soil properties, which vary spatially and temporally due to weather conditions. Importantly, precipitation increases soil water content and blocks gas pathways through the soil, which results in decreasing gas leak emissions to the atmosphere. On the other hand, emissions from a pipeline leak can dry the above soil layer and generate cavities and gas transport channels, which result in temporarily higher emission rates to the surface compared to rates at the leak (Bonnaud et al., 2018). When comparing results from the suction method, which quantifies underground pipeline leakages, to the mobile and tracer methods, which quantify the emissions into the atmosphere, we make the implicit assumption that the emission is in steady state. With this assumption, the different methods can be compared without considering impact of soil conditions. Note that in this study, the weather was mostly dry with few rainy days in August 2020.

S.5) Gas leak detection and quantification methods overview

In theory, emissions from different sources can occur at the same surface location, e.g., at a manhole, and overlap. For combination of fossil and microbial sources, the mixture of fossil with microbial gas would lead to a reduction in the C_2:C_1 ratio which also leads to an overestimate of fossil emissions if the mixture was exclusively attributed to gas leak sources. We attempted to use the C_2:C_1 ratio for a possible correction, but the G4302 instrument showed day-to-day variability even when measuring gas from a cylinder on different days, so we consider this approach not reliable. This is because for the purpose of separating a possible contribution of emission from a microbial source at a specific location in mobile method, it is necessary to quantify reliably small percentage differences from the ratio reported by the LDC in the analysis.

S.5.1) Detection and attribution of locations

We used two methods to report the C_2:C_1 ratio, the single point and the linear method. The single point method calculates the C_2:C_1 ratio from only the maximum of C_2H_6 and CH_4, while the linear method determines the correlation of multiple points of C_2H_6 and CH_4 in a plume. The distance to the leak locations were determined using the location of CH_4 enhancement maxima during the mobile method to the leak location reported by the LDC.

Table S4 - Attribution of individual plumes from mobile measurements using C_2H_6 and CO_2 signals

ID	Leak observation probability (%) from the car based on C_2:C_1 (%)		Attribution at outlet			Leak confirmed by the LDC; Yes (Y), No (N)	CO_2 attribution for transects with CH_4 enhancements > 10%		
	Point method	Linear method	C_2:C_1 (%)	Distance to the leak (m)	Max CH_4 (ppm) (Outlet type)		Transects with CO_2 observ.	CH_4:CO_2 (ppb ppm^{-1})	CO_2 Enhance. (ppm)
HH001	30	0	4.0 – 5.8	≈ 3	≈ 25 (Straight from ground)	Y	0 out of 1	-	-
HH002	60	50	3.4 – 5.3	≈ 3	≈ 230 (Straight from ground)	Y	1 out of 5	240	11
HH003	83	50	2.3 – 3.1	3 - 20	>> 1000 (Tele. cover)	Y	2 out of 6	275 and 180	113 and 8
HH004	75	75	1.5 – 3.5	4 - 17	>> 1000 (Tele. cover)	Y	0 out of 4	-	-
HH005	60	30	1.4 – 5.9	5 - 27	≈ 870 (manhole)	Y	1 out of 19	0.8	260
HH006	40	17	3.0 – 5.2	4 - 33	435 (Curb cracks)	Y	1 out of 11	370	3
HH007	14	0	- ($R^2 < 0.7$)	- (Not confirmed)	4.4 (Pavement cracks)	N	-	-	-
HH008	44	9	4.8 – 6.2	≈ 4	≈ 930 (Hydrant cap)	Y	0 out of 6	-	-
HH009	38	13	1.3 – 4.5	2 - 35	≈ 800 (Rain drain)	Y	1 out of 9	19	235
HH010	38	0	2.3 – 2.4	≈ 2	≈ 65 (Hydrant cap)	Y	0 out of 3	-	-
HH011	38	0	1.9 – 2.8	≈ 60	≈ 70 (Rain drain)	Y	0 out of 4	-	-
HH012	0	0	4.2	-	7.3	N	-	-	-

				(Not confirmed)	(Manhole)				
HH013	40	20	2.6 – 5.0	≈ 15	11.5 (Straight from ground)	Y	0 out of 2	-	-
HH014	55	41	2.3 – 7.2	0 - 11	>> 1000 (Asphalt holes; LDC)	Y	1 out of 24	4000	1.5
HH015	83	33	6.0 – 6.9	≈ 5	> 1000 (Curb cracks)	Y	0 out of 1	-	-
HH100	13	0	1.3 – 2.0	≈ 8	15 (Gas cap)	Y	0 out of 1	-	-
HH101	33	0	2.5	≈ 3	25 (Asphalt holes; LDC)	Y	-	-	-
HH102	33	0	2.2	≈ 1	55 (Asphalt holes; LDC)	Y	-	-	-
HH103	43	0	- ($R^2 < 0.7$)	≈ 1	8 (Asphalt holes; LDC)	Y	-	-	-
HH104	40	0	- ($R^2 < 0.7$)	≈ 1	45 (Asphalt holes; LDC)	Y	-	-	-

S.5.1) Quantifications of locations

Table S5 - Measurement overview of the mobile, tracer and suction methods

ID	Mobile method						Tracer method			Suction method	
	Measurements status; Complete (CPLT)	Number of Transects			Driving Speed (m s^{-1})	Min. driv. track dist. to leak loc. (m)	Measurements status Complete (CPLT)	Release location Right (R), Wrong (W), Questionable (Q)	Acetylene release rate (L min^{-1})	Measurements status; Complete (CPLT), Incomplete (INC)	Pumping rate (L min^{-1}) - time (hr)
		All	Accepted								
			with G2301	with G4302							
HH001	CPLT	10	10	10	3.5±0.8	2.7±1.8	CPLT	R	1.8	INC	-
HH002	CPLT	10	10	10	3.7±0.8	2.4±2.2	CPLT	R	1.8	INC	380 - 6
HH003	CPLT	7	7	6	2.5±2.0	3.0±1.3	CPLT	R	1.6	-	-
HH004	CPLT	4	4	4	1.3±1.1	5.7±2.3	CPLT	Q	1.5	-	-
HH005	CPLT	40	37	37	1.3±1.0	5.5±6.2	CPLT	R	1.5	-	-
HH006	CPLT	31	28	30	3.9±2.0	7.8±7.8	CPLT	Q	2.1	CPLT	345 - 7
HH007	CPLT	8	7	7	2.2±0.7	7.3±3.9	-	-	-	-	-
HH008	CPLT	23	23	23	5.1±3.0	9.3±8.2	CPLT	R	1.3	INC	370 - 10
HH009	CPLT	25	24	24	8.4±4.0	30±14	CPLT	W	1.8	INC	-
HH010	CPLT	8	8	8	3.3±2.0	12±9.7	CPLT	R	1.6	INC	400 - 7
HH011	CPLT	8	8	8	5.9±2.0	25±6.3	CPLT	W	1.4	-	-
HH012	CPLT	4	3	3	5.6±3.0	2.8±1.2	-	-	-	-	-
HH013	CPLT	5	5	5	3.9±2.0	3.2±1.8	-	-	-	-	-
HH014	CPLT	44	44	44	2.7±1.0	13±5.9	CPLT	R	2.3	-	-
HH015	CPLT	6	2	6	3.4±0.8	2.9±1.6	CPLT	R	1.4	INC	380 - 9.5
HH100	CPLT	8	8	8	3.4±3.0	3.3±4.1	CPLT	R	2.6	-	-

HH101	CPLT	6	6	6	3.1±2.0	2.8±1.0	CPLT	R	2.1	INC	240 - 9
HH102	CPLT	6	6	6	8.7±1.0	3.3±1.8	CPLT	R	2.6	-	-
HH103	CPLT	7	7	7	2.3±1.0	3.4±1.0	CPLT	R	1.3	-	-
HH104	CPLT	5	5	5	1.8±1.0	2.4±2.2	-	-	-	-	-

S.6) Gas leak influence on urban vegetation

Increased soil CH_4 content can also adversely influence vegetation. Methanotrophs oxidize CH_4 which lowers the soil oxygen content and consequently impacts soil quality and urban vegetation health (Schollaert et al., 2020). We observed on several occasions that the vegetation, especially trees, next to the leak locations were affected by the presence of a gas leak in proximity. Fig. S12 shows two examples from HH004 and HH010 where trees where affected by gas leaks.

Figure S8 - Example of unhealthy trees (red box) affected by a gas leaks in close vicinity, HH004 (a) and HH010 (b)

S.7) Leak localization

Figure S9 - The LDC reported 6 leaks on the pipeline at this location with total leak area of 5 cm^2, HH013

S.8) Comparison of two CRDS instruments, G2301 and G4302

S.8.1) Comparison of maximum CH_4 enhancements and plume area

Fig. S10 shows the comparison of the maximum CH_4 enhancement recorded during individual transects (Fig.S10a) and the integrated peak area (Fig. S10b) between the two different instruments, G2301 and G4302, which both sampled air from the same inlet at the front bumper.

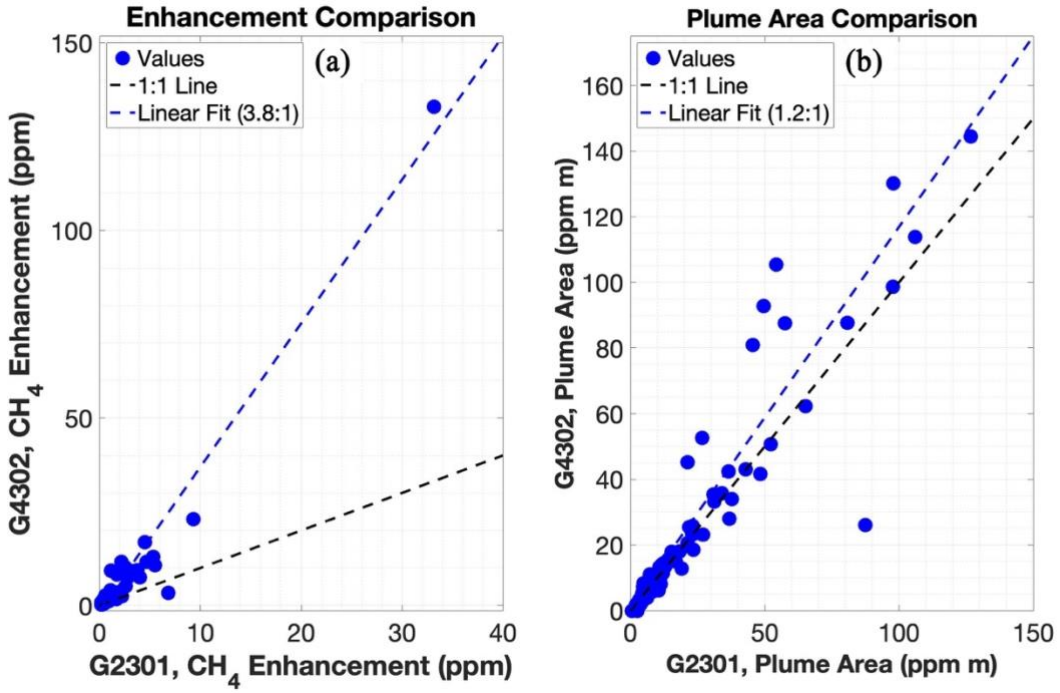

Figure S10 - comparison between maximum CH4 enhancements (a) and plume areas (b) from two different instruments, G2301 and G4302.

S.8.2) Detection of leak indications with two instruments

In Table S6, observations carried out with the G2301 and G4302 instruments are compared. It is shown that the probability of identifying a CH_4 leak indication with the G4302 is generally higher than for the G2301. This is because CH_4 enhancements on the G4302 is 3.8 times higher than enhancements on the G2301 (Fig. S10a).

Table S6 - Observation comparison of CH_4 enhancements from G2301 and G4302

	ID	**G2301** flowrate of ≈ 0.2 L min^{-1} Sampling frequency of ≈ 0.3 Hz Cell size of 35 mL		**G4302** flowrate of ≈ 2.2 L min^{-1} Sampling frequency of ≈ 1 Hz Cell size of 35 mL	
		Transect (s) w/ CH_4 Enh. > 10% threshold	Transects where the G2301 was in operation	Transect (s) w/ CH_4 Enh. > 10% threshold	Transects where the G4302 was in operation
Detected by mobile method	HH001	n = 1 (10%)	n = 10	n = 6 (60%)	n = 10
	HH002	n = 5 (50%)	n = 10	n = 5 (50%)	n = 10
	HH003	n = 6 (86%)	n = 7	n = 6 (100%)	n = 6
	HH004	n = 4 (100%)	n = 4	n = 4 (100%)	n = 4
	HH005	n = 19 (51%)	n = 37	n = 25 (68%)	n = 37

	HH006	n = 11 (39%)	n = 28	n = 17 (57%)	n = 30
	HH007	n = 0 (0%)	n = 7	n = 1 (14%)	n = 7
	HH008	n = 6 (26%)	n = 23	n = 9 (39%)	n = 23
	HH009	n = 9 (38%)	n = 24	n = 10 (42%)	n = 24
	HH010	n = 3 (38%)	n = 8	n = 3 (38%)	n = 8
	HH011	n = 4 (50%)	n = 8	n = 7 (88%)	n = 8
	HH012	n = 0 (0%)	n = 3	n = 1 (33%)	n = 3
	HH013	n = 2 (40%)	n = 5	n = 4 (80%)	n = 5
	HH014	n = 24 (55%)	n = 44	n = 27 (61%)	n = 44
	HH015	n = 1 (50%)	n = 2	n = 6 (100%)	n = 6
Reported by LDC	HH100	n = 1 (13%)	n = 8	n = 4 (50%)	n = 8
	HH101	n = 0 (0%)	n = 6	n = 0 (0%)	n = 6
	HH102	n = 0 (0%)	n = 6	n = 1 (17%)	n = 6
	HH103	n = 0 (0%)	n = 7	n = 2 (29%)	n = 7
	HH104	n = 0 (0%)	n = 5	n = 0 (0%)	n = 5

S.8.3) Emission quantification comparisons

Table S7 - Emission quantification comparison with two different instruments. The G2301 is similar to the instrument that was used to derive the conversion equation (Eq. 1 in the main manuscript, Weller et al, 2019). The G4302 has a much shorter sample exchange time of the measurement cell, therefore, higher enhancements, which translate to higher emission rates if the same conversion equation (Eq. 1) is used for quantification.

	ID	**G2301** flowrate ≈ 0.2 L min^{-1} Sampling frequency of ≈ 0.3 Hz Cell size of 35 mL		**G4302** flowrate ≈ 2.2 L min^{-1} Sampling frequency of ≈ 1 Hz Cell size of 35 mL	
		Emission ave. (L min^{-1})	Emission range (L min^{-1})	Emission ave. (L min^{-1})	Emission range (L min^{-1})
Detected by mobile method	HH001	0.7	-	0.8	0.5 – 1.3
	HH002	4.9	0.7 – 35.1	14.8	3.3 – 67.6
	HH003	7.5	1.4 – 243.5	9.4	0.9 - 1300
	HH004	7.8	2.6 – 22.1	18.1	5.9 – 67.8
	HH005	1.8	0.5 – 51.5	3.3	0.5 – 155.8
	HH006	1.2	0.7 – 5.9	1.7	0.6 – 12.2
	HH007	-	-	0.6	-
	HH008	1.5	0.5 – 16.9	2.5	0.6 – 52.1
	HH009	3.9	0.5 – 21.2	5.9	0.6 – 106.6
	HH010	1.6	0.6 – 2.9	2.8	1.6 – 3.8
	HH011	1.9	0.5 – 14.8	2.0	0.8 – 50.4
	HH012	-	-	0.9	-
	HH013	1.8	1.1 – 3.0	2.6	0.8 – 12.8
	HH014	1.6	0.5 – 27.0	3.1	0.5 – 61.5
	HH015	1.0	-	1.6	0.9 – 3.3
Reported	HH100	0.7	-	1.0	0.7 – 1.2
	HH101	-	-	-	-

	HH102	-	-	0.5	-
	HH103	-	-	0.8	0.7 – 0.9
	HH104	-	-	-	-

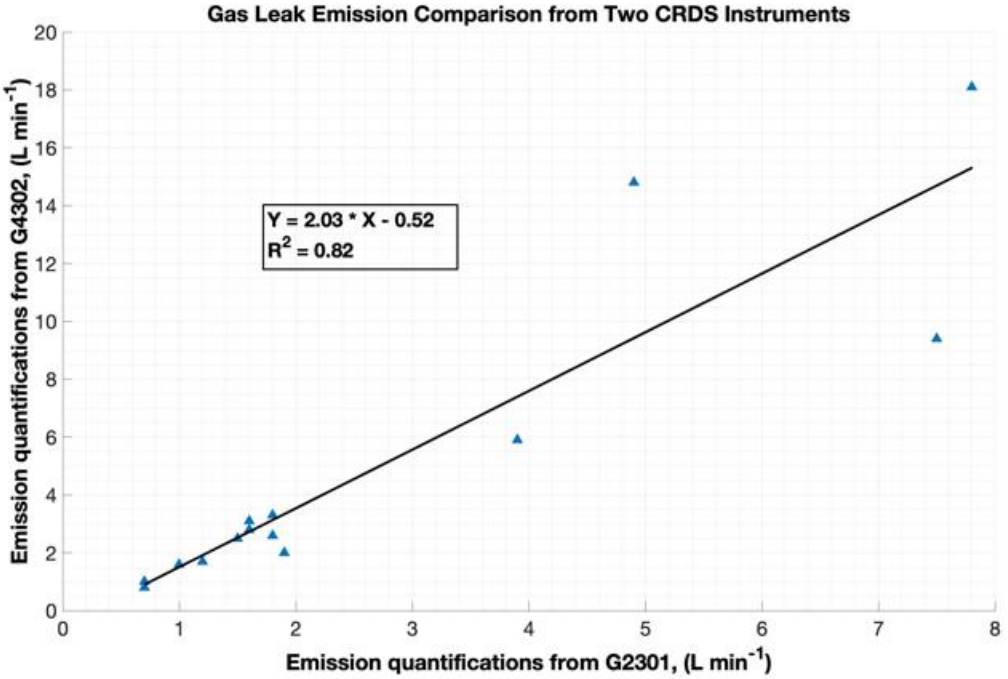

Figure S11 - Emission comparison between the two CRDS instruments, G2301 and G4302, onboard the mobile measurement vehicle

S.9) Impact of distance on the enhancements

Since emission plumes dilute as they disperse through the atmosphere, we expected that the closer the air intake is to the emission point the higher CH_4 enhancements are recorded. Fig. S12 shows the maximum enhancement of individual transects as a function of distance from the actual leak location. The highest CH_4 maxima are observed within 15 to 20 m to the leak locations.

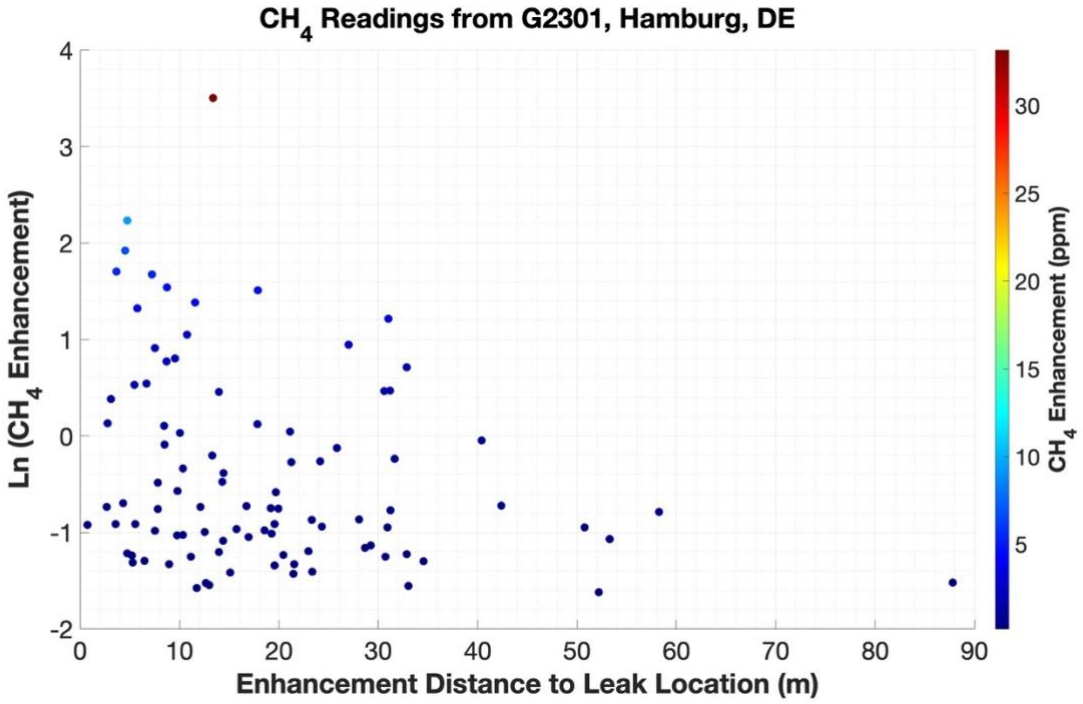

Figure S12 - Impact of distance on the measurements during mobile measurements

S.10) Use of 10% or 10 ppb threshold

Table S8 - Emission estimate for the C_2H_2 release rate from 5 mobile quantifications in the tracer release technique. These were evaluated a) with the original 10% (≈ 200 ppb) threshold and b) with a 10 ppb threshold. The lower threshold was still applied in order to exclude transects where the plume is completely missed.

ID	10% threshold		10 ppb threshold		C_2H_2 actual release rate (L min^{-1})
	C_2H_2 release estimate (L min^{-1})	Distance (m)	C_2H_2 release estimate (L min^{-1})	Distance (m)	
HH008	0.88 (n = 4)	35.5 ± 7.1	0.30 (n = 14)	33.6 ± 4.9	1.29
HH009	0.71 (n = 1)	43.4 ± 30.0	0.05 (n = 16)	49.9 ± 30.0	1.78
HH010	1.51 (n = 10)	44.3 ± 19.7	0.06 (n = 26)	48.0 ± 17.7	1.55
HH011	0.64 (n = 5)	34.5 ± 7.2	0.15 (n = 22)	36.9 ± 9.4	1.38
HH014	2.42 (n = 10)	-	0.86 (n = 16)	-	2.29

S.11) Descriptions of locations that were not described in detail in the main text

S.11.1) HH003

HH003 was at a T-junction of two streets, each of them was about 6 m wide. We detected several outlets with CH_4 signals from which we could also observe ethane signals. The street cover on this location was asphalt. A ≈ 1.5 m stroke with trees separated pavements from streets on both sides. We accepted 7 transects from the mobile measurements for the quantification. The tracer team quantified this location using in static mode ≈ 25 m downwind the release point. The leak had to be fixed immediately after confirmation by the LDC and the suction method could not be applied.

On-foot measurements across the T-junction with the G4302 instrument indicated that emissions from gas leak (s) were mostly released out of four major outlets, including direct emissions from the soil next to a tree, from a manhole, asphalt cracks in the middle of the T-junction and a telecommunication cover. The C_2:C_1 ratio was highest at the telecommunication cover (3.1%, R^2 = 0.91 and max CH_4 reading of >1000 ppm). The ratio of C_2:C_1 next to the tree was 2.4% (R^2 of 0.92 and max CH4 reading of ≈ 22 ppm) with air intake of ≈ 5 cm distance from the soil. The air intake from the asphalt cracks in the middle of the T-junction showed a C_2:C_1 ratio of 2.3% (R^2 of 0.85 and maximum CH_4 reading of ≈ 17 ppm). From the manhole, C_2H_6 signals were observable but the R^2 of the C_2:C_1 linear regression was below 0.7, however CH_4 mole fraction reading went up to of ≈ 27 ppm.

Emission quantification for this location from the mobile measurement method based on the 6 transects with CH_4 enhancement maxima above the 10% threshold on the G2301 was 7.5 L min^{-1}. For HH003, based on the first field assessment, the leak location was assumed to be next to a tree at the T-junction, and the C_2H_2 release was performed with a release rate of 1.55 L min^{-1}. HH003 was listed as type A1 leak by the LDC. The pipeline was DN100ST and in operation since 1963, and the latest inspection of this pipeline was in 2019. The pipeline at this location was replaced completely, 34 m.

S.11.2) HH004

At the end of an almost circular dead-end, 15 m diameter turning bay covered with asphalt, we detected numerous outlets with clear fossil C_2:C_1 ratio (Fig. 1). The turning bay was surrounded by grass and trees and then residential buildings. We found CH_4 and C_2H_6 signals in numerous manholes, rain drains, telecommunication covers, curb cracks and asphalt cracks. As this location was located at a dead-end location, normal driving conditions could not be applied, and after data quality check we considered 4 transects for quantification.

We identified numerous outlets in a circular area with diameter of ≈ 30 m. The maximum CH_4 mole fractions were observed at the telecommunication cover (>> 1000 ppm) which was ≈ 17 m away from the leak location and showed C_2:C_1 ratios of 2.6% (R^2 of 0.99) and 3.3% (R^2 of 0.90) on two different days. Two rain drains which were about 3.8 m and 6.9 m far from the leak location showed C_2:C_1 ratios of 1.5% (R^2 of 0.97, CH_4 maximum 69 ppm) and 2.2% (R^2 of 0.98, CH_4 maximum 110 ppm). The closest outlets with the highest C_2:C_1 ratios of 3.5% (R^2 of 0.99) were several curb cracks, ≈ 5.9 m away from the leak location, and the maximum CH_4 mole fraction at 2-5 cm distance from these cracks was ≈ 30 ppm.

All of the four transects showed CH_4 enhancement higher than 10% above background level. The emission rate derived from mobile measurements was 7.8 L min^{-1} (95% confidence range: 1.8 – 34.5 L min^{-1}). At HH004, the static tracer method was applied ≈ 50 m downwind the release point and an emission rate of 5.3 L min^{-1} was derived. We note that the application of the tracer method is uncertain at this location due to the presence of several outlets, which would qualify the emission rate estimate as a lower limit. Nevertheless, despite the challenging location, at HH004 there was a good agreement of the two "above ground" emission rate estimates, confirming the existence of a relatively large leak. Unfortunately, the suction method could not be applied at HH004 because of the widespread CH_4 soil accumulation in close vicinity to residential buildings, so this leak (category A1) had to be fixed immediately.

S.11.3) HH005

In the beginning of a ≈ 4.5 m wide street, we observed CH_4 and C_2H_6 signals on several days. In total we had 37 accepted transects for this location from the mobile measurement. The street cover was asphalt with two soil-covered pavements on each side, one was ≈ 2.5 m wide and the other one was ≈ 1 m wide. The houses at this location had front yards, some were separated from street with bushes but there were not big trees around the leak area. Comparing to other locations like HH003, this location was not very confined with buildings. The LDC reported three leaks over a ≈ 30 m distance of the street, and we used the average latitude and longitude coordinates as the representative location for this location. We identified several outlets at this location and considered the "strongest" outlet as the main emission point. The tracer team applied static quantification and due to time constraint, suction team could not be deployed at this location.

Several outlets along about 30 m segment of the street were identified as fossil emitting points including two manholes rain drains and curb cracks. There was a manhole in the middle and another one at the pavement. The manhole in the middle of the road which was ≈ 5.5 m far from the representative location of the leak showed C_2:C_1 ratios of 2.0% (R^2 of 0.8, max CH_4 of ≈ 29 ppm), 3.1% (R^2 of 0.88 and max CH_4 of ≈ 890 ppm), 4.6% (R^2 of 0.99 and max CH_4 of ≈ 20 ppm) and 3.3% (R^2 of 0.92 and max CH_4 of ≈ 16 ppm) on different days. The other manhole located on the pavement which was ≈ 9.5 m far from representative leak location showed C_2:C_1 ratios of 3.6% (R^2 of 0.98 and max CH_4 of ≈ 67 ppm) and 2.4% (R^2 of 0.98 and max CH_4 of ≈ 9 ppm) on two different days. There were many different curb cracks. Some examples: At 9.5 m distance to the representative leak location with C_2:C_1 of 4.1% (R^2 of 0.91, max CH_4 of ≈ 60 ppm), 7 m far from the representative location with C_2:C_1 ratio of 1.4% (R^2 of 0.85 and max CH_4 of ≈ 100 ppm), at a distance of ≈ 5 m with C_2:C_1 ratio of 4.8% (R^2 of 0.97 and max CH_4 of ≈ 320 ppm) and the other location at distance of ≈ 6 m and C_2:C_1 ratio of 5.9% (R^2 of 0.96 and max CH_4 of ≈ 170 ppm). Fossil emissions were also observed from three rain drains with C_2:C_1 ratios of 4.6% (R^2 of 0.98, distance of 26 m and max CH_4 of ≈ 110 ppm) 5.6% (R^2 of 0.99, distance of 12 m and max CH_4 of ≈ 100 ppm) and 5.3% (R^2 of 0.98 distance of 23 m and max CH_4 of ≈ 720 ppm).

From the 20 transects, out of 37 transects, which showed CH_4 mole fraction more than 10% above background level on G2301, the leak rate was estimated 1.8 L min^{-1} from mobile method. The tracer method was applied for this location with C_2H_2 at the "strongest" emission location. CH_4 and C_2H_6 plumes were measured in static mode at 40 m. The emission rate derived for this location from the tracer method was 0.2 L min^{-1} from the tracer method. All the three leaks found at this location were categorized as A2, on DN80ST pipeline, and happened due to corrosion. The reported leak areas were ≈ 1 cm^2 for one and ≈ 5 cm^2 for the other two leaks. For the two leaks with leak area of ≈ 5 cm^2, 6 - 7 m segments of the pipeline were replaced. The emission estimates for the smaller hole were 19 L min^{-1} and 39 L min^{-1} for the bigger holes from the hole model.

S.11.4) HH006

About 25 m from a T-junction, we found strong signals mainly coming out of street curbs and also from some of the gaps between pavement bricks. The asphalt street was ≈ 5 m wide with a ≈ 1 m pavement on one side and several trees close to each other on the other side. For this location the LDC reported two leaks, one of the leaks was in the middle of the T-junction and the other one was ≈ 25 m far away. The first one was repaired during the campaign, but we could still detect signals after the repair. After revisits with the LDC, we detected the second leak, and we assume that the second leak was there for the whole period. Bush walls existed on both side of the street. Mobile measurements performed 28 transects on this location. The tracer method was applied in static mode for this location. The suction method could quantify this location completely. Both tracer and suction methods were applied to the second leak as the first leak had been already fixed.

The highest CH_4 mole fraction was observed from the street curbs with ratio of 5.2% (R^2 of 0.92 and max CH_4 of ≈ 440 ppm). C_2:C_1 ratio from the pavement cracks with air inlet of 2-5 cm above ground level was 4.9% (R^2 of 0.78 and max CH_4 reading of ≈ 110 ppm). We also observed C_2:C_1 ratio of 3.3% (R^2 of 0.9 and max CH_4 reading of 3.8 ppm) from two manholes very close to each other (≈ 1 m) but about 25 m far from the leak location. The manholes were closer to the first leak location, but we could still observe C_2H_6 and CH_4 signals even after repair of the first leak.

The emission rate estimate from the mobile measurements at this location was 1.2 L min^{-1}. This includes signals from 11 transects (out of 28) which showed CH_4 mole fraction maxima above the 10% threshold on the G2301 instrument. The tracer method was applied in static mode at ≈ 15 m distance from the leak location. The emission rate of 0.02 L min^{-1} was derived from the tracer method. The suction method was applied for this location successfully and the emission estimated emission rate was ≈ 0.3 L min^{-1}.

The first leak was classified as A1 and had to be repaired immediately and the second leak was classified as B. The pipeline of the first leak was documented as DN80ST while the pipeline of the second leak was bigger with code DN100ST. Both pipelines were steel and dated back to 1934. The leaks on both locations were due to corrosion. The first leak had ≈ 0.5 cm^2 area while the second leak had ≈ 2 cm^2 leak area, which respectively were translated to 12 L min^{-1} and 33 L min^{-1} from the hole method.

S.11.5) HH009

On a T-junction of a 6 m wide street and a bigger road next to a fuel station we found several outlets. On both sides of the smaller street, there were ≈ 2 m wide pavements. Based on the visit together with the LDC, initially "two" leak locations were indicated with ≈ 20 m distance from each other, but later after opening the ground no leak evidence was found at one of the locations. So, for this location the actual leak location was about 20 m north of the T-junction into the smaller road. The bigger road was ≈ 15 m wide at the T-junction and it was a two-way street with heavier traffic than the one-way and smaller street. Both streets had an asphalt surface. In the southeast corner of the T-junction there was a gas station and on the northwest corner of the T-junction there were some shops and a 3 - 4 m wide pavement. Next to the leak, there was a tree and no vegetation was present. We detected emissions mainly from two rain drains, a manhole and pavement cracks next to the wrongly assigned leak location. At this location, the mobile measurement was applied, the tracer method was also applied at the initially assumed leak location and the suction method was applied for one day at the first location but in the second day on the second location (≈ 20 m far from the first location) where the LDC found the actual leak location. As this location showed several outlets far from each other, similar to one other location (HH011), we included all CH_4 enhancements within 100 m radius of the leak location.

On-foot measurements of outlets at this location showed that major emissions were released to the atmosphere through two gullies, ≈ 11 m apart, on two sides of smaller street, a manhole and some cracks on pavement. The C_2:C_1 ratio from the gully closest to the leak (≈ 2 m) was 4.5% (R^2 of 0.93 with max CH_4 of ≈ 800 ppm) and 3.3% (R^2 of 0.31 and max CH4 of ≈ 360 ppm) on two different days. The C_2:C_1 ratio from the other gully (≈ 13.5 m far from the leak) was 2.4% (R^2 of 0.92 and max CH_4 of 18 ppm) and 2.5% (R^2 of 0.92 with max CH_4 of ≈ 280 ppm) on two different days. The C_2:C_1 ratio from the manhole with ≈ 4.5 m distance to the leak was 3.1% (R^2 of 0.84 and max CH_4 of ≈ 730 ppm). The C_2:C_1 ratio from the pavement cracks was 1.3% (R^2 of 0.7 with max CH_4 of ≈ 16 ppm).

Based on the CH_4 enhancements from 9 transects which showed enhancements more than 10% above background level on the G2301 instrument, the emission rate estimate from the mobile method was 3.9 L min^{-1}. For HH009, the tracer method was applied in mobile mode, and the CH_4 emission rate estimate for this location from the tracer method was 4.9 L min^{-1}. The suction method estimated an upper-limit emission rate of 3 L min^{-1} for this location based on incomplete measurements. The LDC classified the leak at this location as A1 category from a DN80ST pipeline which was installed in 1928.

S.11.6) HH010

On a ≈ 4.5 m wide one way street, we detected signals of gas leak (s). On both side of the street there were about 2 – 3 m wide pavements with trees on both sides. Buildings were separated by small gardens from the pavements. On the east side of the street, there was no gap between side-to-side houses, while on the west side of the street, there was a recreational area with a line of trees. The fossil signals were detected mainly from a hydrant cap and bare soil next to a tree. The street cover was asphalt and pavement the was covered with cobblestones. The hydrant and tree were about ≈ 1 m far apart.

Emissions from the hydrant showed signals with C_2:C_1 ratio of 2.4% (R^2 of 0.77 and max CH_4 mole fraction of 20 ppm) and signals from bare soil next to a tree, ≈ 1m far from the hydrant cap, showed a C_2:C_1 ratio of 2.3% (R^2 of 0.94 and max CH_4 mole fraction of 65 ppm).

Based on the three CH_4 enhancements which were more than 10% above background level on the G2301, the CH_4 emission rate for this location was estimated 1.6 L min^{-1}. The tracer method was applied in mobile mode and estimated an emission rate of 0.5 L min^{-1}. The suction method reported an emission rate of 0.7 L min^{-1} for this location. This location was classified as type C leak location. The pipeline was DN200ST and dated back to 1937. Pipeline overpressure is 30 – 60 mbar. Due to presence of a large tree it was not possible to dig at the assumed leak location and 30 m of pipeline was replaced.

S.11.7) HH012

On a 6-m wide and two-way street, we found a manhole which showed methane and ethane signals on some days but not on the other days. The leak detection expert from the LDC didn't confirm any leak in the vicinity of this outlet which was similar to the situation of HH007. We had 3 accepted transects for this location from mobile measurements, but we didn't apply the tracer and suction methods as the gas leak on this location was not confirmed.

On-foot measurements with G4302 showed C_2:C_1 ratio of 4.2% (R^2 of 0.82) with max CH_4 mole fraction of 7.3 ppm from the manhole.

None of the CH_4 signals from G2301 were above the 10% threshold, so it is not possible to quantify the emission rate for this location from mobile measurements with the standard approach. The tracer and suction methods were not applied at this location as no gas leak was confirmed from the LDC surveys.

S.11.8) HH013

On a ≈ 3-m wide street we detected signals of gas leak emissions. On both sides of the street there were pavements with bare soil, and on the side where we also detected signals there were some shallow canals (≈ 0.5 m deep). Very few trees grew on each side of the street and houses were separated by short bushes from the street.

We performed several transects at this location, but before applying the tracer or suction method the gas leak had been found by routine surveys of the LDC independently and was fixed before applying suction or tracer methods.

On-foot surveys of the area with the G4302 showed a C_2:C_1 ratio of 5.0% (R^2 of 0.85 and max CH_4 mole fraction of 5.8 ppm) at 2-5 cm distance from ground.

Based on the two CH_4 enhancements, which were more than 10% above background level on G2301, the emission rate 1.8 L min^{-1} was derived for this location. The leak was classified as A1 leak from a DN80ST pipeline which dated back to 1939 with overpressure of 30 – 60 mbar. The total leak area, 6 holes (See Sect. S.7) next to each other, was estimated ≈ 5 cm^2 which was due to corrosion.

S.11.9) HH014

During mobile surveys, at a T-junction of two streets, we passed a location that had been already detected by the LDC and was under repair procedures. The ground was already open with safety fences around the location. Both streets were ≈ 5 m wide and on both sides, there were strokes with about 1 m wide bare soil. There were trees and bushes on both sides of the streets, including a tree ≈ 2 m away from the leak location. There were dispersed houses with private gardens around this location and buildings were less dense compared to most of other locations, e.g. HH003. We performed mobile measurements and tracer release at this location, but as the ground was already open, it was not possible to apply the suction method.

The recorded C_2:C_1 ratio from the open ground area with some soil on top of the pipeline was 7.2% (R^2 of 0.95 and max CH_4 enhancement of 94 ppm). The C_2:C_1 ratio from two holes in asphalt with distance of ≈ 9 and ≈ 11 m to the leak location were 2.3% (R^2 of 0.93 and max CH_4 of ≈ 330 ppm) and 3.2% (R^2 of 0.99 and max CH_4 of >>1000 ppm).

Out of the 44 transects, CH_4 enhancements from 24 transects exceeded the 10% threshold on the G2301 instrument, which then were used to quantify the emission rate, yielding an emission rate estimate of 1.5 L min^{-1}. The tracer method was applied for this location in mobile mode and estimated an emission rate of 1.4 L min^{-1}.

This leak was categorized as A1 leak on a DN100St pipeline, which had been in operation since 1950, the leak area was estimated as ≈ 5 cm^2 as a result of corrosion. For this location, 12 m of gas pipeline were subsequently replaced by the LDC. Previous inspection for this location was in 2016. Gas overpressure of this pipeline, like other locations, was between 30 – 60 mbar.

S.11.10) HH015

On a ≈ 4.5-m wide street, we detected signals of fossil CH_4, which then was confirmed as a gas leak location by the LDC. The street cover was asphalt and on both sides of the street, there were ≈ 2 m wide pavements. Emissions were coming mainly from two manholes close to each other in the middle of the street and several curb cracks along ≈ 5 m length of pavement on one side of the street. For this location, we had 6 transects but due to technical issues, the G2301 instrument was not in operation for 4 transects, however the G4302 was available in all of the 6 transects. For the quantification, we only used the measurement from the two transects when G2301 was running, while for the attribution we report measurements during all transects (n = 6) from G4302.

Two manholes, ≈ 1 m apart from each other were identified as outlets, and also the curb cracks of the pavement above the leaky pipeline. The C_2:C_1 ratios measured from the manholes were similar with values of 6.0% (R^2 of 0.99 and max CH_4 of ≈ 270 ppm) and the C_2:C_1 ratio from the cracks was 6.9% (R^2 of 0.91 and max CH_4 of >1000 ppm).

Based on the only two transects for this location from mobile measurements when the G2301 was in operation, the emission estimate for this location was 0.6 L min^{-1}. The tracer method was applied in static mode at ≈ 20 m downwind the release location. The emission rate estimate from the tracer method for was 0.4 L min^{-1}. The suction method was applied for this location, and based on the incomplete measurements, the emission rate estimate was estimated ≈ 0.9 L min^{-1}. This leak was classified as an A1 leak from a DN80ST pipeline dated back to 1935. For this location, two of the connections were leaking and a corrosion leak area of ≈ 1 cm^2 was reported by the LDC. To repair this location, ≈ 10 m of pipeline was replaced.

S.11.11) HH100

This location was one of the five leak locations reported by the LDC. The emissions were coming through several gas cap outlets located in asphalt. The road was a bit elevated relative to the surrounding area with dispersed houses and open agricultural fields around. Compared to most of the first 15 locations (HH001 – HH015), this location had very open surroundings. For this location, we had quantification from mobile measurements and tracer method.

On-foot measurements of the surrounding area with the G4302 instrument resulted in finding 4 gas caps next to each other as the emission source. The C_2:C_1 ratios measured at two of these caps were 2.0% (R^2 of 0.83 with max CH_4 mole fraction of 14.9 ppm) and 1.3% (R^2 of 0.81 with max CH_4 mole fraction of 11.4 ppm). For the other two, the linear regression between C_2H_6 and CH_4 was insufficient to derive a reliable estimate.

Only two of the transects at this location showed CH_4 enhancements above the 10% threshold, and an emission rate of 0.6 L min^{-1} was derived from mobile measurements. The static measurements of released C_2H_2 and CH_4 plumes were performed ≈ 30 m downwind C_2H_2 release point, the center of the gas caps, with release rate of 2.6 L min^{-1}. The emission rate estimate of the tracer method for this location was 0.14 L min^{-1}. Due to time constraints, the suction method was not deployed at this location.

This location was classified as C category and the leak was a d225Pe pipeline dated back to 1994. The latest inspection of this area was in 2016.

S.11.12) HH102

On one side of the two-lane asphalt road, the LDC reported a gas leak. This was a ≈ 6 m wide road with a narrow, ≈ 1 m wide, pavement on one side. On the both sides of the leak location there were trees and bushes, but beyond the vegetation line there were open fields and few scattered houses one the south side of the road.

The LDC had already drilled holes in the ground on top of the pipeline during their routine surveys and these holes were identified as the only emission outlets with C_2:C_1 ratio of 2.2% (R^2 of 0.91) and max CH_4 mole fraction of 55 ppm.

None of the CH_4 enhancements on G2301 were above the 10% threshold, thus no quantification could be derived from the mobile measurement technique using the "standard algorithm". The tracer method was applied at this location in static mode at ≈ 20 m distance from the release location and the estimated emission rate was 0.01 L min^{-1}. The suction method was not performed due to time constraints. The leak at this location was classified as C category from a DN125ST pipeline which was operational since in 1928. The overpressure at this location was 30 – 60 mbar, similar to the other location.

S.11.13) HH103

This leak was found by the LDC on a ≈ 4.5 m wide cobblestone street. On the east side of the street, there was a ≈ 2 m wide bare soil pavement and on the other side there was a narrow, ≈ 1 m wide, asphalt pavement. The leak was located on the east side of the street, where in about 3 m distance there were some bushes. The location was widely open and there were not dense buildings around.

The C_2H_6 signals from the location didn't give a good correlation with CH_4 so no C_2:C_1 ratio could be derived for this location.

As none of the CH_4 enhancements on G2301 was greater than the 10% threshold, we couldn't report gas emission for this location from mobile measurement "standard" method. The tracer method quantified this location in static mode at ≈ 18 m distance from the release location and estimated an emission rate of 0.03 L min^{-1}. Due to time constraints, the suction method was not applied at this location.

This location was classified as B category from a DN150ST pipeline which was connected to the distribution network in 1963.

S.11.14) HH104

On a 5-m wide asphalt covered street south-east of Hamburg municipality with about 1 m pavement on both sides, the LDC reported another leak location. The were some houses around the street but beyond the houses there were agricultural fields. There were private open spaces between houses.

None of CH_4 enhancements from any of the transects exceeded the 10% threshold, so based on the mobile measurements it's not possible to report emission rate for this location. At the time of applying the tracer method, CH_4 emission signals could not be detected at the reported location, thus tracer release was not applied. The suction method was also not applied due to time limitation.

The leak was categorized as C category from a DN100ST pipeline which was installed and connected to gas network in 1930. The pipeline overpressure for this location was 30 – 60 mbar.

References

Bonnaud, C., Cluzel, V., Corcoles, P., Dubois, J. P., Louvet, V., Maury, M., Narbonne, A., Orefice, H., Perez, A., Ranty, J., Salim, R., Zeller, L. M., Foissac, A., Poenou, J., Experimental study and modelling of the consequences of small leaks on buried transmission gas pipeline, Journal of Loss Prevention in the Process Industries, 55, 303-312, https://doi.org/10.1016/j.jlp.2018.06.010, 2018.

Cho, Y., Ulrich, B. A., Zimmerle, D. J., Smits, K. M., Estimating natural gas emissions from underground pipelines using surface concentration measurements, Environmental Pollution, https://doi.org/10.1016/j.envpol.2020.115514, 2020.

Ebrahimi-Moghadam, A., Farzaneh-Gord, M., Arabkoohsar, A., Jabari Moghadam, A., CFD analysis of natural gas emission from damaged pipelines: Correlation development for leakage estimation, Cleaner Production, https://doi.org/10.1016/j.jclepro.2018.07.127, 2018.

Fredenslund, A. M., Rees-White, T. C., Beaven, R. P., Delre, A., Finlayson, A., Helmore, J., Allen, G., Scheutz, C.: Validation and error assessment of the mobile tracer gas dispersion method for measurement of fugitive emissions from area sources, Waste Management, 83, 68-78, https://doi.org/10.1016/j.wasman.2018.10.036, 2019.

Maazallahi, H., Fernandez, J. M., Menoud, M., Zavala-Araiza, D., Weller, Z. D., Schwietzke, S., von Fischer, J. C., Denier van der Gon, H., and Röckmann, T.: Methane mapping, emission quantification, and attribution in two European cities: Utrecht (NL) and Hamburg (DE), Atmos. Chem. Phys., 20, 14717–14740, https://doi.org/10.5194/acp-20-14717-2020, 2020.

Schollaert, C., Ackley, R. C., DeSantis, A., Polka, E., & Scammell, M. K., Natural gas leaks and tree death: A first-look case-control study of urban trees in Chelsea, MA USA. Environmental Pollution, 263. https://doi.org/10.1016/j.envpol.2020.114464, 2020.

Weller, Z. D., Yang, D. K., and von Fischer, J. C.: An open source algorithm to detect natural gas leaks from mobile methane survey data, edited by: Mauder, M., PLoS One, 14, e0212287, https://doi.org/10.1371/journal.pone.0212287, 2019.